Arthritis & Rheumatology
Vol. 76, No. 6, June 2024, pp 882–893
DOI 10.1002/art.42815
© 2024 The Authors. *Arthritis & Rheumatology* published by Wiley Periodicals LLC on behalf of American College of Rheumatology.
This is an open access article under the terms of the Creative Commons Attribution-NonCommercial-NoDerivs License, which permits use and distribution in any medium, provided the original work is properly cited, the use is non-commercial and no modifications or adaptations are made.

American College of Rheumatology
Empowering Rheumatology Professionals

Predisposal of Interferon Regulatory Factor 1 Deficiency to Accumulate DNA Damage and Promote Osteoarthritis Development in Cartilage

Yongsik Cho,[1] Hyeonkyeong Kim,[1] Geunho Yook,[2] Sangmin Yong,[2] Soy Kim,[2] Narae Lee,[2] Yi-Jun Kim,[3] Jin-Hee Kim,[4] Tae Woo Kim,[5] Moon Jong Chang,[5] Kyoung Min Lee,[5] Chong Bum Chang,[6] Seung-Baik Kang,[5] and Jin-Hong Kim[7]

Objective. Interferon regulatory factor 1 (IRF1) is a transcriptional regulator conventionally associated with immunomodulation. Recent molecular analyses mapping DNA binding sites of IRF1 have suggested its potential function in DNA repair. However, the physiologic significance of this noncanonical function remains unexplored. Here, we investigated the role of IRF1 in osteoarthritis (OA), a condition marked by senescence and chronic joint inflammation.

Methods. OA progression was examined in wild-type and *Irf1*$^{-/-}$ mice using histologic assessments and microcomputed tomography analysis of whole-joint OA manifestations and behavioral assessments of joint pain. An integrated analysis of assay for transposase-accessible chromatin with sequencing and whole transcriptome data was conducted for the functional assessment of IRF1 in chondrocytes. The role of IRF1 in DNA repair and senescence was investigated by assaying γ-H2AX foci and senescence-associated beta-galactosidase activity.

Results. Our genome-wide investigation of IRF1 footprinting in chondrocytes revealed its primary occupancies in the promoters of DNA repair genes without noticeable footprint patterns in those of interferon-responsive genes. Chondrocytes lacking IRF1 accumulated irreversible DNA damage under oxidative stress, facilitating their entry into cellular senescence. IRF1 was down-regulated in the cartilage of human and mouse OA. Although IRF1 overexpression did not elicit an inflammatory response in joints or affect OA development, genetic deletion of *Irf1* caused enhanced chondrocyte senescence and exacerbated post-traumatic OA in mice.

Conclusion. IRF1 offers DNA damage surveillance in chondrocytes, protecting them from oxidative stress associated with OA risk factors. Our study provides a crucial and cautionary perspective that compromising IRF1 activity renders chondrocytes vulnerable to cellular senescence and promotes OA development.

INTRODUCTION

Interferon regulatory factor 1 (IRF1) is a transcriptional regulator with canonical roles in the immune response and host defenses.[1] As inflammation is a central process contributing to symptoms and disease progression in arthritis, IRF family proteins have been studied in joint tissues, underscoring their roles in activating immune cells and producing inflammatory cytokines.[2] During the pathogenesis of rheumatoid arthritis, IRF1 mediates the expression of tumor necrosis factor–induced genes in endothelial cells[3] and fibroblast-like synoviocytes,[4,5] contributing to the recruitment of macrophages and the initiation of inflammatory processes in mice.[6]

Supported by the National Research Foundation of Korea (grants NRF-2023R1A2C3003864 and NRF-2021R1I1A1A01059252); the Korea Drug Development Fund funded by the Ministry of Science and information & communication technology (ICT), Ministry of Trade, Industry, and Energy, and Ministry of Health and Welfare (grant RS-2023-00217266); the Institute for Basic Science from the Ministry of Science, ICT, and Future Planning of Korea (grant IBS-R008-D1); the Ministry of Education of Korea (grant 2021RIS-001); and the Suh Kyungbae Foundation.

[1]Yongsik Cho, PhD, Hyeonkyeong Kim, PhD: Institute for Basic Science and Seoul National University, Seoul, South Korea, and Liflex Science, Cheongju, South Korea; [2]Geunho Yook, BS, Sangmin Yong, BS, Soy Kim, BS, Narae Lee, BS: Institute for Basic Science and Seoul National University, Seoul, South Korea; [3]Yi-Jun Kim, MD, PhD: Ewha Womans University, Seoul, South Korea; [4]Jin-Hee Kim, PhD: Cheongju University, Cheongju, South Korea; [5]Tae Woo Kim, MD, PhD, Moon Jong Chang, MD, PhD, Kyoung Min Lee, MD, PhD, Seung-Baik Kang, MD, PhD: Seoul National University and Boramae Hospital, Seoul, South Korea; [6]Chong Bum Chang, MD, PhD: Seoul National University Bundang Hospital, Seongnam, South Korea; [7]Jin-Hong Kim, PhD: Seoul National University and Institute for Basic Science, Seoul, South Korea, and Institute of Green-Bio Science and Technology, Pyeongchang, South Korea.

Drs Cho, H. Kim, and Yook contributed equally to this work.

Additional supplementary information cited in this article can be found online in the Supporting Information section (https://acrjournals.onlinelibrary.wiley.com/doi/10.1002/art.42815).

Author disclosures and graphical abstract are available at https://onlinelibrary.wiley.com/doi/10.1002/art.42815.

Address correspondence via email to Jin-Hong Kim, PhD, at jinhkim@snu.ac.kr.

Submitted for publication April 26, 2023; accepted in revised form January 23, 2024.

Osteoarthritis (OA) is the most common form of arthritis, mainly characterized by progressive degeneration of articular cartilage. OA involves low-grade chronic inflammation that is distinct from the inflammatory process of rheumatoid arthritis.[2,7] OA primarily involves pathologic transition of chondrocytes, a major resident cell type in articular cartilage.[8] Chondrocytes are inevitably exposed to the risk of mechanical overload linked to generating reactive oxygen species (ROS).[9] The accumulation of ROS causes permanent DNA damages in chondrocytes and promotes their senescence.[10–14] Senescent chondrocytes in osteoarthritic cartilage secrete various proinflammatory cytokines, chemokines, and matrix-degrading enzymes, collectively referred to as senescence-associated secretory phenotypes (SASPs).[15] SASPs aggravate chronic inflammation in a non–cell-autonomous manner by stimulating neighboring chondrocytes and synoviocytes, accelerating OA progression.[16]

Here, we reveal that IRF1 plays a distinct chondroprotective role in the cartilage, independent of its conventional immunomodulatory functions. IRF1 offers DNA damage surveillance in chondrocytes, protecting them from oxidative stress generated during load-bearing events in articular cartilage. Genetic deletion of *Irf1* results in the failure of such surveillance mechanisms and the accumulation of senescent chondrocytes, thereby accelerating the development of post-traumatic OA in mice. It is imperative to note the noncanonical yet physiologically relevant role of IRF1 in the DNA damage response in the context of age-related diseases such as OA.

MATERIALS AND METHODS

A detailed description of the procedures and specific materials used for histology and immunohistochemistry, primary culture of mouse articular chondrocytes, microcomputed tomography (μCT) analysis, animal behavioral test, assay for transposase-accessible chromatin with sequencing (ATAC-seq), peak calling from ATAC-seq data, ATAC-seq footprint analysis, transcriptomic analysis, induction of DNA damage and cellular senescence in chondrocytes, adenovirus infection of chondrocytes, reverse transcription polymerase chain reaction (PCR) and quantitative real-time PCR, antibodies, bone volume (BV/TV) and subchondral bone plate thickness (Subcho.BP.Th) assessment, immunofluorescence, comet assay, and senescence-associated beta-galactosidase (SA-β-Gal) staining are provided in the Supplementary Materials and Methods. PCR primers are summarized in Supplementary Table 1.

Human cartilage. Human cartilage tissues were obtained from patients with OA who underwent total knee arthroplasty at Seoul National University Boramae Medical Center. The Boramae Medical Center Institutional Review Board (IRB) reviewed and approved the collection of human specimens (IRB 30-2017-48). Seoul National University IRB reviewed and approved the study design concerning the use of the specimens (IRB E1803/003-009). Written informed consent was obtained from all participants before the total knee replacement arthroplasty operative procedure. Formalin-fixed paraffin-embedded blocks of normal human cartilage were obtained from OriGene (CB806018, CB807297, CB807500, and CB810351).

Experimental OA in mice. Wild-type (WT) C57BL/6 mice were purchased from Daehan Biolink. *Irf1*$^{-/-}$ mice were obtained from Jackson Laboratory. All animal experiments were approved by the Seoul National University Institutional Animal Care and Use Committee (SNU-190311-3-1). We conformed to the Animal Research: Reporting of In Vivo Experiments guidelines for reporting animal experiments.[17] Destabilization of the medial meniscus (DMM) surgery was performed on the right knee of 12-week-old male mice to induce post-traumatic OA. A sham operation was used as a control.[18] The mice were sacrificed, and their knee joints were processed two, four, six, and eight weeks after surgery to conduct histologic and immunostaining analyses. To evaluate skeletal development, histologic analysis of the knee joint was performed at postnatal day zero on WT and *Irf1*$^{-/-}$ mice. We used intra-articular (IA) injection of adeno-associated virus (AAV) for in vivo overexpression of IRF1 in joints. Plasmid(p)AAV-Cytomegalovirus promoter (CMV) vectors expressing enhanced green fluorescent protein (e*GFP*), *Irf1*, and pHelper were purchased from Takara Bio USA. The serotype 9 Rep/Cap plasmid was purchased from Addgene. e*GFP* or mouse *Irf1* complementary DNA was cloned into the pAAV-CMV vector. AAV-e*GFP* or AAV-*Irf1* was produced by triple transfection of AAVpro 293T cells (Takara Bio USA) according to the manufacturer's protocol. After AAV-e*GFP* or AAV-*Irf1* was titrated using an AAVpro titration kit (Takara Bio USA), AAV-e*GFP* or AAV-*Irf1* was administered by IA injection to 12-week-old male mice. A total of 2.0×10^8 AAV particles were injected into the mice in a volume of 10 μL phosphate-buffered saline. The mice received weekly injections of AAV particles for either two or three weeks. They were then sacrificed at four or eight weeks after the initial injection for RNA extraction and histologic analysis.

Statistical analyses. All experiments were conducted independently at least thrice. Data are expressed as the mean ± SEM. A parametric test based on a two-tailed unpaired Student's *t*-test or a nonparametric test based on the Mann–Whitney *U* test was used to compare the two groups. To compare multiple groups and repeated measures, a parametric test based on one-way analysis of variance followed by Fisher's least significant difference test and a nonparametric test based on the Kruskal–Wallis test followed by the Mann–Whitney *U* test were used. For the transcriptomic analysis, the Wald test followed by Benjamini–Hochberg correction was used with the DESeq2 R package. Statistical significance was set at $P < 0.05$. GraphPad Prism 9.1.0 was used for all the statistical analyses, except for transcriptomic analysis.

RIGHTSLINK

23265205, 2024, 6, Downloaded from https://acrjournals.onlinelibrary.wiley.com/doi/10.1002/art.42815 by Ewha Womans University Library, Wiley Online Library on [30/10/2024]. See the Terms and Conditions (https://onlinelibrary.wiley.com/terms-and-conditions) on Wiley Online Library for rules of use; OA articles are governed by the applicable Creative Commons License

RESULTS

IRF1 is down-regulated in OA cartilage. We initially examined the expression of IRF1 in the articular cartilage of patients with knee OA to elucidate the potential association between IRF1 and OA development. Immunohistochemical analysis showed that IRF1 expression was observed in all layers of normal cartilage and the undamaged region of OA cartilage (Figure 1A–C). However, IRF1 positivity in the superficial, middle, and deep zones of the damaged OA cartilage was reduced to 23%, 52%, and 51% of that of the undamaged cartilage, respectively (Figure 1C). Reduced IRF1 levels were also observed in mouse cartilage affected by post-traumatic OA induced by DMM surgery when compared with levels in naive and sham-operated mice (Figure 1D–F). IRF1 expression was decreased in the meniscus of DMM-operated mice compared with the sham group, mirroring the trends observed in the articular cartilage (Supplementary Figure 1A and B). In the synovium, IRF1 expression was overall low in both the sham and DMM groups (Supplementary Figure 1A and B). The analysis of the publicly available transcriptome data set in cartilage from humans with OA (GSE114007) and from a mouse model of DMM-induced OA at various time points (GSE41342) indicated a significant reduction in IRF1 messenger RNA levels in these OA cartilage samples (Supplementary Figure 1C and D). Collectively, IRF1 expression was consistently reduced during the development of OA in both human and mouse cartilage.

Interestingly, the DMM-induced down-regulation of IRF1 expression preceded the onset of severe cartilage destruction, suggesting a possible causative link between IRF1 down-regulation and OA development. Notably, the regulation of IRF1 expression was independent of interferons (IFNs) in chondrocytes. IFNα and IFNγ did not alter the expression of IRF1, although they robustly activated the signal transducer and activator of transcription 1 (STAT1) pathway (Figure 1G–L). IFN stimulation did not elicit the expression of matrix-degrading enzymes such as a disintegrin and metalloproteinase with thrombospondin motifs 5 (ADAMTS5) or matrix metalloproteinase 13 (MMP13); IFNγ mildly elevated interleukin-6 (IL-6) expression at a high dose (Figure 1G and J). Similarly, IL-1β did not alter the expression of IRF1, and IL-1β–mediated expression of catabolic enzymes was not affected by the knockdown of IRF1 (Supplementary Figure 1E and F).

IRF1 overexpression does not cause joint inflammation and OA in mice. IRF1 did not influence the inflammatory responses of chondrocytes in the presence of proinflammatory cytokines such as IFNs or IL-1β (Figure 1G–L and Supplementary Figure 1E and F). To directly assess the function of IRF1 in chondrocytes, we overexpressed IRF1 in primary cultured chondrocytes using an adenoviral system.

Primary cultured mouse chondrocytes were infected with adenovirus-expressing mouse *Irf1* (Ad-*Irf1*) at doses of 200, 400, and 800 multiplicities of infection (MOI) and, for comparison, with 800 MOI of adenovirus-expressing e*GFP* (Ad-e*GFP*). We observed a dose-dependent increase in IRF1 expression (Figure 2A and B). The moderate overexpression of IRF1 achieved with 200 and 400 MOI of Ad-*Irf1* did not induce the expression of inflammatory mediators (*Nos2* and *Ptgs2*), matrix-degrading enzymes (*Adamts5* and *Mmp13*), or proinflammatory cytokine (*Il6*) in chondrocytes (Supplementary Figure 2A and B). A notably significant elevation of IRF1 was observed at the 800 MOI of Ad-*Irf1* (Figure 2C). Under this condition, the expressions of inflammatory mediators such as *Nos2* and *Ptgs2* showed a slight increase, whereas those of matrix-degrading enzymes such as *Adamts5* or *Mmp13*, as well as proinflammatory cytokine such as *Il6*, remained unaltered (Figure 2D and Supplementary Table 2).

The in vivo effect of IRF1 overexpression was directly examined by IA injection of the AAV encoding *Irf1* (AAV-*Irf1*) (Supplementary Figure 2C). The confirmation of successful gene delivery to mouse articular cartilage via this system was established by introducing AAV carrying e*GFP* (AAV-e*GFP*), a gene that is not endogenously expressed in mice (Supplementary Figure 2D). A substantial overexpression of IRF1 was achieved in articular cartilage both at the transcript and protein levels, at four and eight weeks after the initial IA injection (Figure 2E–J). However, under these experimental schemes, IRF1 overexpression did not result in the emergence of OA phenotypes, such as cartilage destruction and subchondral bone sclerosis (Figure 2K and L). Despite a significant overexpression of IRF1 in the synovium, there was no apparent synovitis observed after the IA delivery of AAV-*Irf1* (Supplementary Figure 2E and F and Figure 2K and L). μCT did not reveal any subchondral bone remodeling in joints after overexpressing IRF1 (Figure 2M). Similarly, overexpression of IRF1 did not induce mechanical allodynia, which was assessed as a pain readout associated with OA in mice (Figure 2N).

Genetic deletion of *Irf1* exacerbates OA development in mice. Next, we examined the pathophysiologic role of IRF1 in OA pathogenesis using *Irf1* knockout ($Irf1^{-/-}$) mice. $Irf1^{-/-}$ mice exhibited normal cartilage development without any significant difference in the relative lengths of the growth plate zones of the developing cartilage on postnatal day zero compared with those of WT mice (Figure 3A and B). We confirmed that the IRF1 protein was completely absent in the knee joint tissues, including articular cartilage, meniscus, synovial membrane, and subchondral bone, of skeletally mature 12-week-old $Irf1^{-/-}$ mice (Figure 3C and Supplementary Figure 3A). We then performed DMM surgery on adult WT and $Irf1^{-/-}$ mice. $Irf1^{-/-}$ mice exhibited augmented OA progression, accelerating cartilage degeneration at both six and eight weeks after DMM surgery (Figure 3D and E and Supplementary Figure 3B–D). Moreover, DMM-operated $Irf1^{-/-}$ mice exhibited significant enhancement of other major OA manifestations, such as

RIGHTSLINK

23265205, 2024, 6, Downloaded from https://acrjournals.onlinelibrary.wiley.com/doi/10.1002/art.42815 by Ewha Womans University Library, Wiley Online Library on [30/10/2024]. See the Terms and Conditions (https://onlinelibrary.wiley.com/terms-and-conditions) on Wiley Online Library for rules of use; OA articles are governed by the applicable Creative Commons License

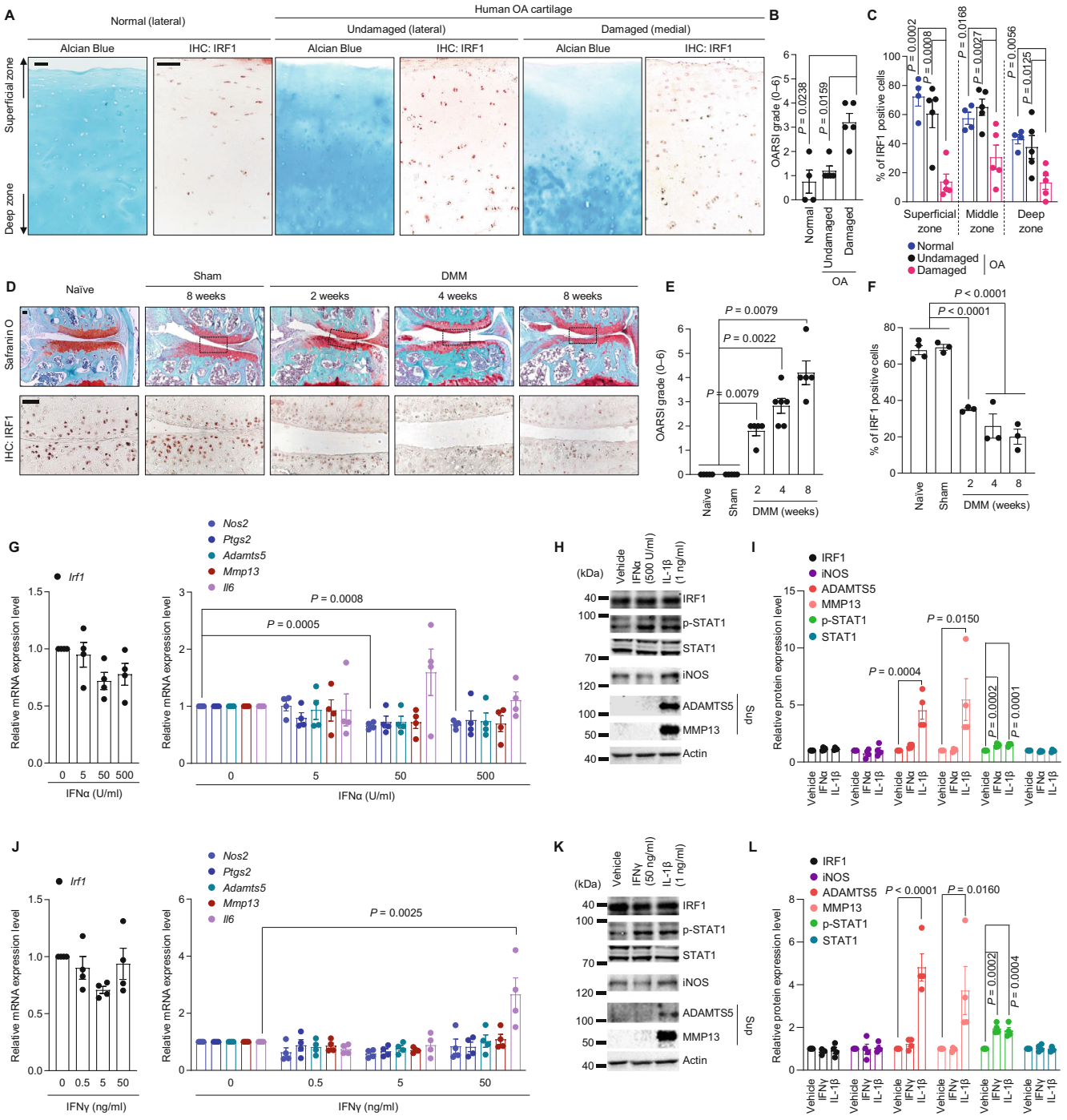


Figure 1. IRF1 is down-regulated in osteoarthritic chondrocytes independent of IFN signaling pathways. (A–C) Representative images of Alcian blue staining with IRF1 IHC (A), corresponding OARSI grades (B), and quantification of IHC in human cartilage (n ≥ 4) (C) are shown. (D–F) Representative images of Safranin O staining (n ≥ 5) with IRF1 IHC (n = 3) (D), corresponding OARSI grades (E), and quantification of IHC in the mouse articular cartilage (F) are shown. (G–I) mRNA and protein levels of the indicated genes in mouse chondrocytes treated with IFNα or IL-1β are shown. qRT-PCR data (n = 4) (G), representative Western blot images (H), and quantification data (n = 4) (I) are given. (J–L) mRNA and protein levels of the indicated genes in mouse chondrocytes treated with IFNγ or IL-1β are shown. qRT-PCR data (n = 4) (J), representative Western blot images (K), and quantification data (n = 4) (L) are given. Data are presented as the mean ± SEM. *P* values were obtained using the Kruskal–Wallis test (B and E) followed by the Mann–Whitney *U* test (C, F, G, I, and J) and ANOVA followed by Fisher's LSD test (L). Scale bars: 100 μm (A) and 50 μm (D). Uncropped Western blot images are in Supplementary Figure 6A. ADAMTS5, a disintegrin and metalloproteinase with thrombospondin motifs 5; ANOVA, analysis of variance; DMM, destabilization of the medial meniscus; IFN, interferon; IHC, immunohistochemistry; IL, interleukin; iNOS, inducible nitric oxide synthase; IRF1, interferon regulatory factor 1; LSD, least significant difference; mRNA, messenger RNA; OA, osteoarthritis; OARSI, Osteoarthritis Research Society International; MMP13, matrix metalloproteinase 13; qRT-PCR, quantitative real-time polymerase chain reaction; Sup, culture supernatant.

RIGHTSLINK

23265205, 2024, 6, Downloaded from https://acrjournals.onlinelibrary.wiley.com/doi/10.1002/art.42815 by Ewha Womans University Library, Wiley Online Library on [30/10/2024]. See the Terms and Conditions (https://onlinelibrary.wiley.com/terms-and-conditions) on Wiley Online Library for rules of use; OA articles are governed by the applicable Creative Commons License

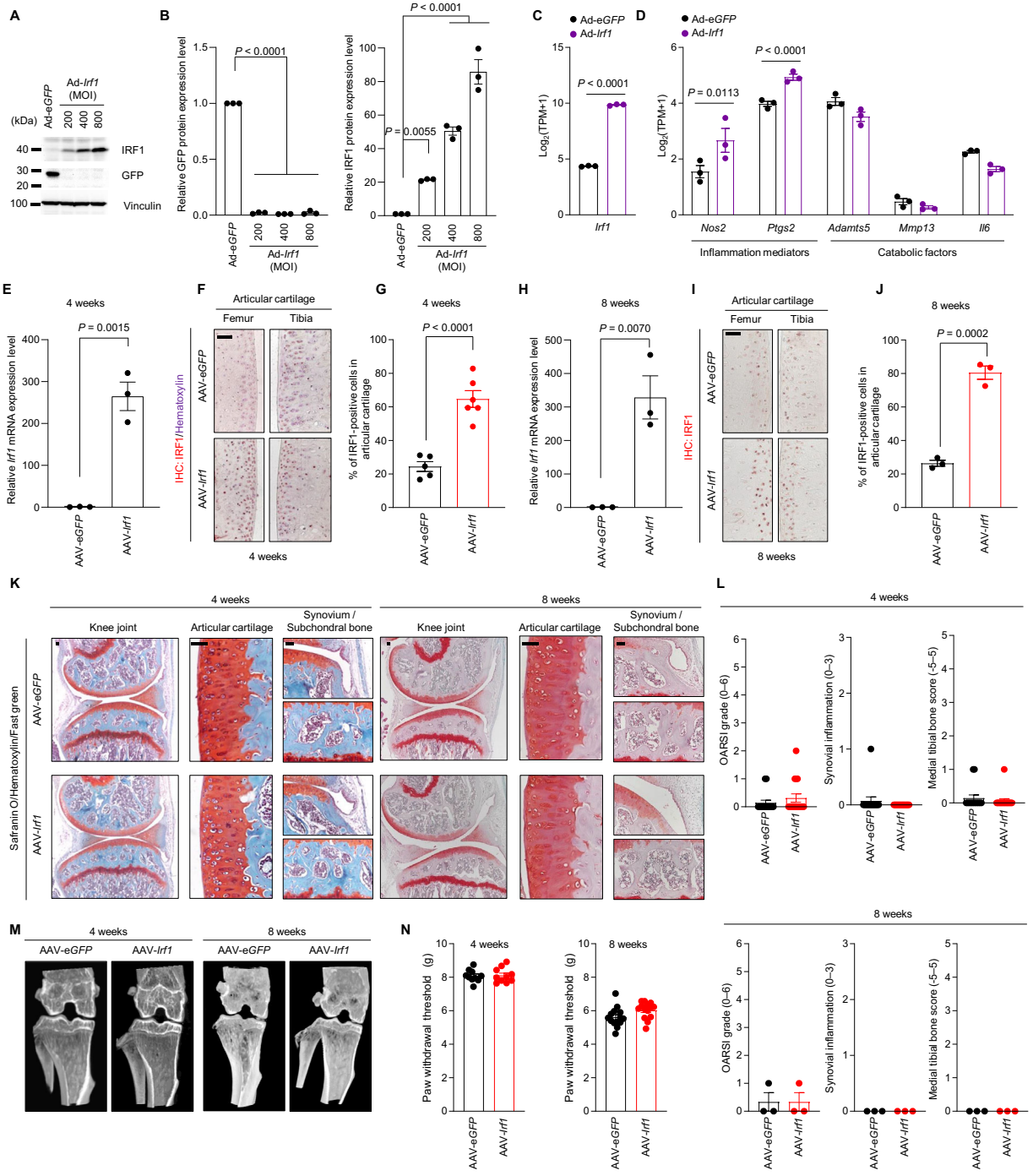


Figure 2. IRF1 overexpression does not affect OA pathogenesis in mice. Representative Western blot images (A) and quantification from mouse chondrocytes infected with Ad-e*GFP* or Ad-*Irf1* (n = 3) (B) are shown. Transcriptomic analysis of mouse chondrocytes infected with Ad-e*GFP* (C) or Ad-*Irf1* (D) at 800 MOI (n = 3) is shown. Transcript levels of *Irf1* (C) and indicated genes (D) are shown. (E–J) IRF1 mRNA and protein levels in mouse articular cartilage after the injections of AAV-e*GFP* or AAV-*Irf1* are given. Relative *Irf*1 expression (n = 3) in four weeks (E) and eight weeks (H) is shown. Representative images and quantification of IRF1 IHC (n ≥ 5) at four weeks (F and G) and eight weeks (n = 3) (I and J) are shown. (K) Representative histology of knee joint from indicated mice is shown. (L) Histologic grading of OA manifestations (n ≥ 3) is shown. (M) μCT of AAV-e*GFP*– or AAV-*Irf1*–injected mice is shown. (N) Withdrawal threshold in the hind paw of indicated mice (n ≥ 10) is shown. Data are presented as the mean ± SEM. *P* values were obtained using ANOVA followed by Fisher's LSD test (B), the Wald test followed by Benjamini-Hochberg correction (C and D), Student's *t*-test (E, G, H, J, and N), and the Mann–Whitney *U* test (L). Scale bars: 50 μm (F, I, and K). Uncropped Western blots are given in Supplementary Figure 6B. AAV, adeno-associated virus; Ad-e*GFP*, adenovirus-expressing green fluorescent protein; ANOVA, analysis of variance; IHC, immunohistochemistry; IRF1, interferon regulatory factor 1; LSD, least significant difference; MOI, multiplicities of infection; mRNA, messenger RNA; OA, osteoarthritis; OARSI, Osteoarthritis Research Society International; μCT, microcomputed tomography.

RIGHTSLINK

23265205, 2024, 6, Downloaded from https://acrjournals.onlinelibrary.wiley.com/doi/10.1002/art.42815 by Ewha Womans University Library, Wiley Online Library on [30/10/2024]. See the Terms and Conditions (https://onlinelibrary.wiley.com/terms-and-conditions) on Wiley Online Library for rules of use; OA articles are governed by the applicable Creative Commons License

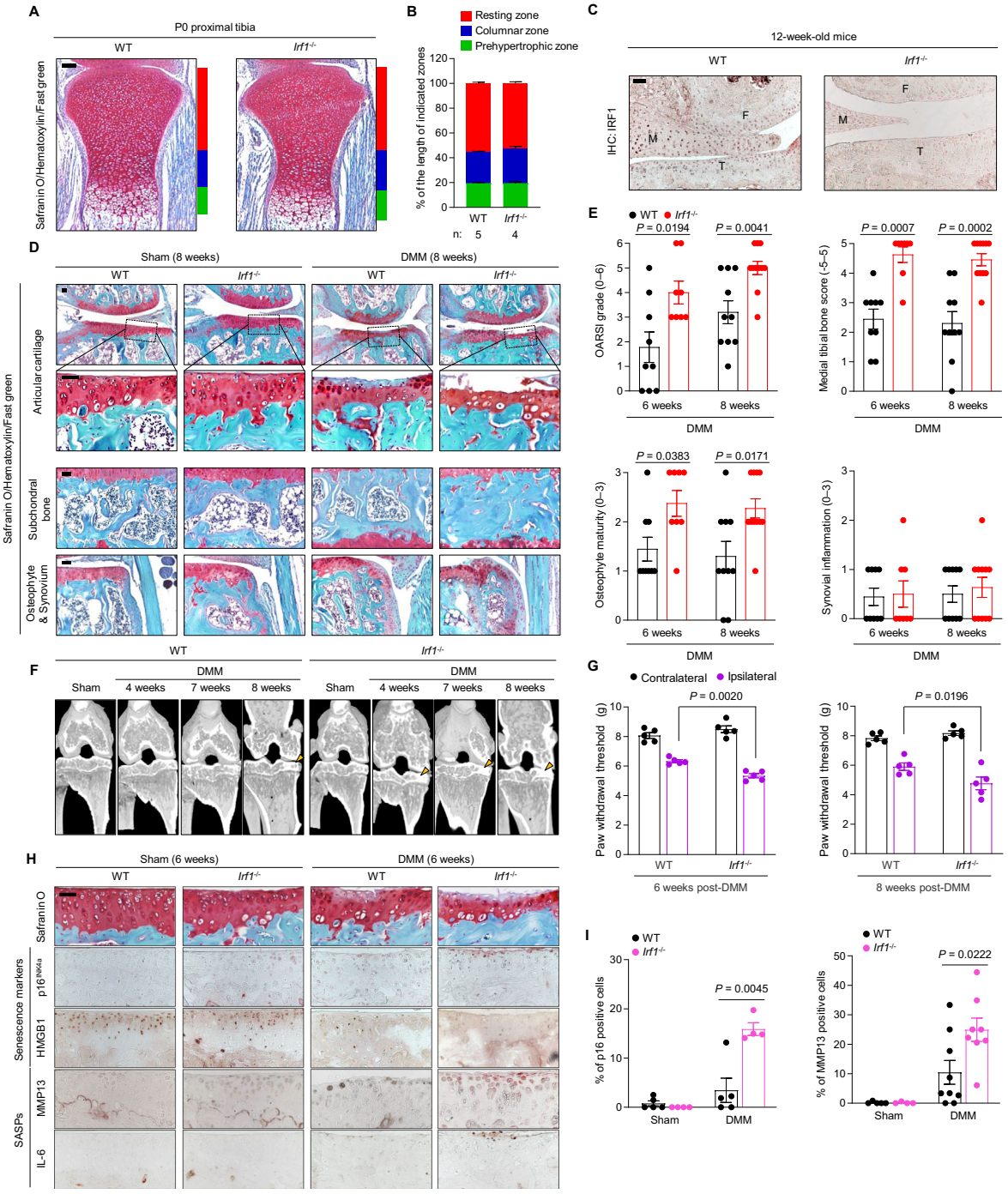


Figure 3. *Irf1* knockout augments post-traumatic OA in mice. (A) Histologic images of the proximal tibial epiphysis from newborn (P0) WT and *Irf1*$^{-/-}$ mice are shown. (B) Relative length of each growth plate zone normalized to the total of the epiphyseal cartilage length (n ≥ 4) is given. (C) Representative IHC images of IRF1 in knee joint from WT and *Irf1*$^{-/-}$ mice are shown. F, femur; M, meniscus; T, tibia. (D) Histology of knee joint from sham- or DMM-operated WT and *Irf1*$^{-/-}$ mice eight weeks post-surgery is shown. (E) Histologic grading of OA manifestations (n ≥ 5) is given. (F) μCT of WT and *Irf1*$^{-/-}$ mice at the indicated time points post-DMM is shown. Yellow arrowheads indicate subchondral sclerosis. (G) Withdrawal thresholds in the hind paw of WT and *Irf1*$^{-/-}$ mice (n = 5) are shown. (H) Histologic and IHC images of knee joint from sham- or DMM-operated WT and *Irf1*$^{-/-}$ mice six weeks post-surgery (n ≥ 4) are shown. (I) Indicated proteins were detected by IHC. Quantitation of p16^{INK4a}- and MMP13-positive cells is given. Data are presented as the mean ± SEM. *P* values were obtained using Student's *t*-test (B and I), the Mann–Whitney *U* test (E), and ANOVA followed by Fisher's LSD test (G). Scale bars: 100 μm (A) and 50 μm (C, D, and H). ANOVA, analysis of variance; DMM, destabilization of the medial meniscus; F, femur; IL, interleukin; HMGB1, high mobility group box 1; IHC, immunohistochemistry; IRF1, interferon regulatory factor 1; LSD, least significant difference; M, meniscus; MMP13, matrix metalloproteinase 13; OA, osteoarthritis; OARSI, Osteoarthritis Research Society International; P0, postnatal day 0; SASPs, senescence-associated secretory phenotypes; T, tibia; WT, wild-type; μCT, micro-computed tomography.

RIGHTSLINK

23265205, 2024, 6, Downloaded from https://acrjournals.onlinelibrary.wiley.com/doi/10.1002/art.42815 by Ewha Womans University Library, Wiley Online Library on [30/10/2024]. See the Terms and Conditions (https://onlinelibrary.wiley.com/terms-and-conditions) on Wiley Online Library for rules of use; OA articles are governed by the applicable Creative Commons License

subchondral bone sclerosis and osteophyte formation (Figure 3D and E and Supplementary Figure 3B–D). In accordance with our histologic evaluations, which revealed substantial elevations in BV/TV and Subcho.BP.Th in *Irf1*$^{-/-}$ mice (Supplementary Figure 3E), μCT analysis of DMM-operated mice across the time course of the experiment indicated that *Irf1*$^{-/-}$ mice displayed markedly accelerated subchondral bone remodeling in the medial tibial plateau compared with WT mice (Figure 3F). Moreover, *Irf1*$^{-/-}$ mice exhibited a marked reduction in the threshold of response to mechanical stimuli, indicating a significant progression of mechanical allodynia (Figure 3G).

In OA, senescent chondrocytes accumulate in the articular cartilage, and SASP factors released by senescent chondrocytes contribute to the breakdown of the cartilage matrix and chronic inflammation in the joints.[10,19] Thus, we examined how *Irf1* knockout affects the senescence of chondrocytes in mice. To detect senescent chondrocytes, the expression of p16^{INK4a} and high mobility group box 1 (HMGB1) were examined in sham- and DMM-operated WT and *Irf1*$^{-/-}$ mice. Nuclear expression of HMGB1 is known to be lost in senescent chondrocytes of OA cartilage.[19] At six weeks after DMM surgery, WT mice exhibited mild-to-moderate OA with a relatively small fraction of senescent cells in their articular cartilage, indicated by the low levels of p16^{INK4a} and nuclear HMGB1 (Figure 3H and I). In contrast, *Irf1*$^{-/-}$ mice displayed a significantly higher fraction of p16^{INK4a}-positive chondrocytes in the superficial zone of the cartilage; furthermore, nuclear localization of HMGB1 was absent in the articular cartilage of *Irf1*$^{-/-}$ mice. Consistent with the increased populations of senescent chondrocytes in DMM-operated *Irf1*$^{-/-}$ mice, their articular cartilage expressed elevated levels of MMP13 and IL-6 (Figure 3H and I), key SASP factors underlying cartilage destruction.[20,21] The elevation of p16^{INK4a} and SASP factors was noticeable in the cartilage of *Irf1*$^{-/-}$ mice as early as four weeks post-DMM, at which WT mice had not shown significant up-regulation of these factors (Supplementary Figure 3F and G). Besides the cartilage in the joint tissues, the meniscus of *Irf1*$^{-/-}$ mice displayed a moderate increase in the expression of p16^{INK4a} and MMP13 (Supplementary Figure 3H). Taken together, our results highlighted the deleterious effects of IRF1 deficiency on OA development.

IRF1 regulates the expression of DNA repair genes, having footprints on their promoters. We set out to investigate the mechanisms underlying the protective role of IRF1 in the development of OA. First, we characterized regulatory elements accessible to IRF1 via DNA footprint analysis in chondrocytes by employing the assay for ATAC-seq (Figure 4A). Because transcription factor (TF)–bound DNA regions are protected from Tn5 transposase cleavage during ATAC-seq, comparing DNA footprints to TF motif databases enables the identification of direct TF-binding sites. We performed footprint analysis across the regulatory regions with open chromatin defined as −3,500 to +500 base pairs from the transcription start sites (Supplementary Figure 4A). We identified 1,262 potential IRF1 target genes by mapping the DNA footprints that overlapped with the binding motifs of IRF1 (Figure 4B and Supplementary Figure 4B–D). We then conducted gene ontology (GO) analysis on the genes containing IRF1 footprints to reveal their functional associations in chondrocytes. The IRF1–footprinted genes were significantly associated with functional annotations related to DNA damage response pathways, such as "RNA methyltransferase activity,"[22] "Damaged DNA binding," "tRNA (cytosine) methyltransferase activity,"[23] and "Lys63-specific deubiquitinase activity"[24] (Figure 4C). To further examine that IRF1 footprints are present in the promoters of DNA damage response genes in chondrocytes, footprinting analysis was selectively performed on the regulatory regions of the target genes. Distinct footprint patterns of IRF1 were identified in the promoter regions of DNA damage-responsive (Figure 4D) and DNA repair (Supplementary Figure 4E) genes. In contrast, no evident footprint patterns were observed in the promoters of IFN-responsive genes (Figure 4E and Supplementary Figure 4F and G). To validate whether IRF1 regulates the expression of DNA repair genes, we performed RNA sequencing (RNA-seq) on chondrocytes transfected with small interfering RNA (siRNA) targeting *Irf1* or control siRNA. Gene set enrichment analysis revealed that the "DNA repair" gene set from GO annotations was negatively enriched in the whole transcriptome of *Irf1* knockdown chondrocytes (Figure 4F). Conversely, DNA repair genes exhibited overall increase upon IRF1 overexpression using adenoviral infection (Supplementary Figure 4H). Next, we conducted an integrated analysis of our bulk RNA-seq and ATAC-seq data. Building upon the identification of genes containing IRF1 footprints through ATAC-seq analysis, our bulk RNA-seq data revealed overall down-regulation of these IRF1–footprinted genes in response to *Irf1* knockdown (Figure 4G and Supplementary Table 3). We further focused on DNA repair–associated genes that possess IRF1 footprints in their promoters. The IRF1–footprinted DNA repair genes such as *Ascc3*, *Helb*, *Smc6*, *Bod1l*, and *Ercc6l* exhibited significant down-regulation upon the knockdown of *Irf1* in primary cultured mouse chondrocytes (Supplementary Figure 4I). Collectively, IRF1 governs the transcriptional regulation of DNA damage response genes in chondrocytes.

IRF1 protects against irreversible DNA damage and senescence in chondrocytes. Chondrocytes are continually exposed to various cellular stressors, including oxidative stress, which can ultimately cause DNA damage,[10,25] underscoring the importance of robust DNA repair mechanisms. Thus, we tested whether IRF1 expression is necessary for mediating DNA repair processes in chondrocytes. The repair kinetics after DNA damage were examined in chondrocytes treated with bleomycin, a DNA-damaging agent. In control siRNA–treated chondrocytes, the γ-H2AX foci positivity significantly decreased after

RIGHTSLINK

23265205, 2024, 6, Downloaded from https://acrjournals.onlinelibrary.wiley.com/doi/10.1002/art.42815 by Ewha Womans University Library, Wiley Online Library on [30/10/2024]. See the Terms and Conditions (https://onlinelibrary.wiley.com/terms-and-conditions) on Wiley Online Library for rules of use; OA articles are governed by the applicable Creative Commons License

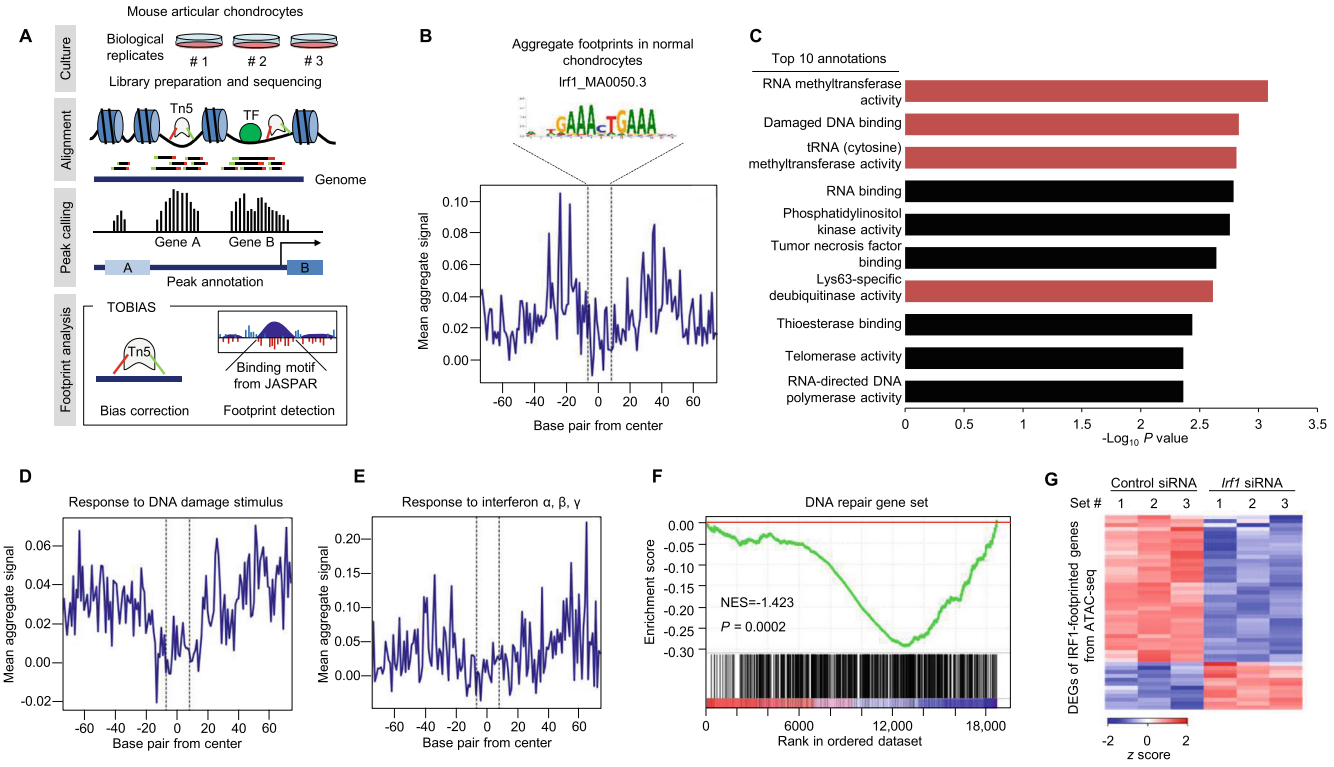


Figure 4. Association of IRF1 footprints with DNA repair genes in chondrocytes. (A) Flowchart of ATAC-seq analysis performed in chondrocytes is given. After three biologic replicates were aligned to a reference genome, peak calling and peak annotation were conducted with merged reads followed by footprint analysis. (B) Aggregated plot for bias-corrected footprints of IRF1 is shown. Mean ATAC-seq signals were centered around a predicted binding motif of IRF1 from JASPAR. (C) Top 10 GO molecular function annotations associated with IRF1–footprinted genes are ranked by *P* values calculated with Fisher's exact test. The red graphs indicate GO annotations related to DNA damage response. (D and E) Footprints of IRF1 in promoter regions of indicated gene sets. ATAC-seq signals were calculated from the GO annotations "Response to DNA damage stimulus" (D) and "Response to interferon α, β, γ" (E), respectively. (F and G) Transcriptomic analysis of *Irf1* knockdown mouse chondrocytes is shown. (F) GSEA result using a "DNA repair" gene set from GO annotations represented with NES and a nominal *P* value is given. (G) Heatmap of IRF1–footprinted DEGs with *z* scores calculated from log-transformed normalized counts is shown. ATAC-seq, assay for transposase-accessible chromatin with sequencing; DEG, differentially expressed gene; GO, Gene Ontology; GSEA, gene set enrichment analysis; IRF1, interferon regulatory factor 1; NES, normalized enrichment score; siRNA, small interfering RNA; TF, transcription factor; tRNA, transfer RNA.

8 hours, indicating that DNA damage was efficiently repaired (Figure 5A and B). In contrast, chondrocytes with *Irf1* knockdown did not exhibit a decrease in γ-H2AX foci positivity over time, resulting in the marked accumulation of DNA damage. We then employed the comet assay to assess DNA damage in chondrocytes after bleomycin exposure, revealing that significant DNA breakage persisted in *Irf1* knockdown cells, in contrast to those treated with control siRNA (Figure 5C and D). Because persistent activation of DNA damage responses leads to cellular senescence,[26] we further examined whether *Irf1* knockdown affects the entry of chondrocytes into a state of senescence. Chondrocytes with *Irf1* knockdown displayed a higher proportion of SA-β-Gal–positive cells after exposure to bleomycin (Figure 5E and F). Consistently, the knockdown of *Irf1* resulted in a significant increase in *Cdkn2a*^{Ink4a} expression in chondrocytes treated with bleomycin (Figure 5G).

Finally, chondrocytes are unavoidably exposed to the risk of mechanical overload, which is associated with the production of ROS.[9] In addition, etiologic OA risk factors, such as aging and obesity, contribute to the disruption of redox homeostasis, resulting in a net increase in cellular ROS. Thus, we examined whether IRF1 was responsible for managing ROS-induced DNA damage. Because chondrocytes originate from low-oxygen physiologic environments,[27] prolonged normoxic exposure induces significant oxidative stress in primary cultured mouse chondrocytes.[10] Notably, we found that the knockdown of *Irf1* markedly facilitated the onset of senescence in chondrocytes cultured under normoxia after a single serial passage, a stage at which chondrocytes treated with control siRNA showed no significant signs of senescence (Figure 5H and Supplementary Figure 5A). Next, we performed a time-course analysis of γ-H2AX in vitro assays using H_2O_2 (Figure 5I and 5J). In chondrocytes treated with control siRNA, the positivity of γ-H2AX foci significantly decreased at 8 hours and continued to decrease at 12 hours, demonstrating efficient DNA damage repair. In contrast, chondrocytes with *Irf1* knockdown did not show a decrease in γ-H2AX foci positivity over

RIGHTSLINK

23265205, 2024, 6, Downloaded from https://acrjournals.onlinelibrary.wiley.com/doi/10.1002/art.42815 by Ewha Womans University Library, Wiley Online Library on [30/10/2024]. See the Terms and Conditions (https://onlinelibrary.wiley.com/terms-and-conditions) on Wiley Online Library for rules of use; OA articles are governed by the applicable Creative Commons License

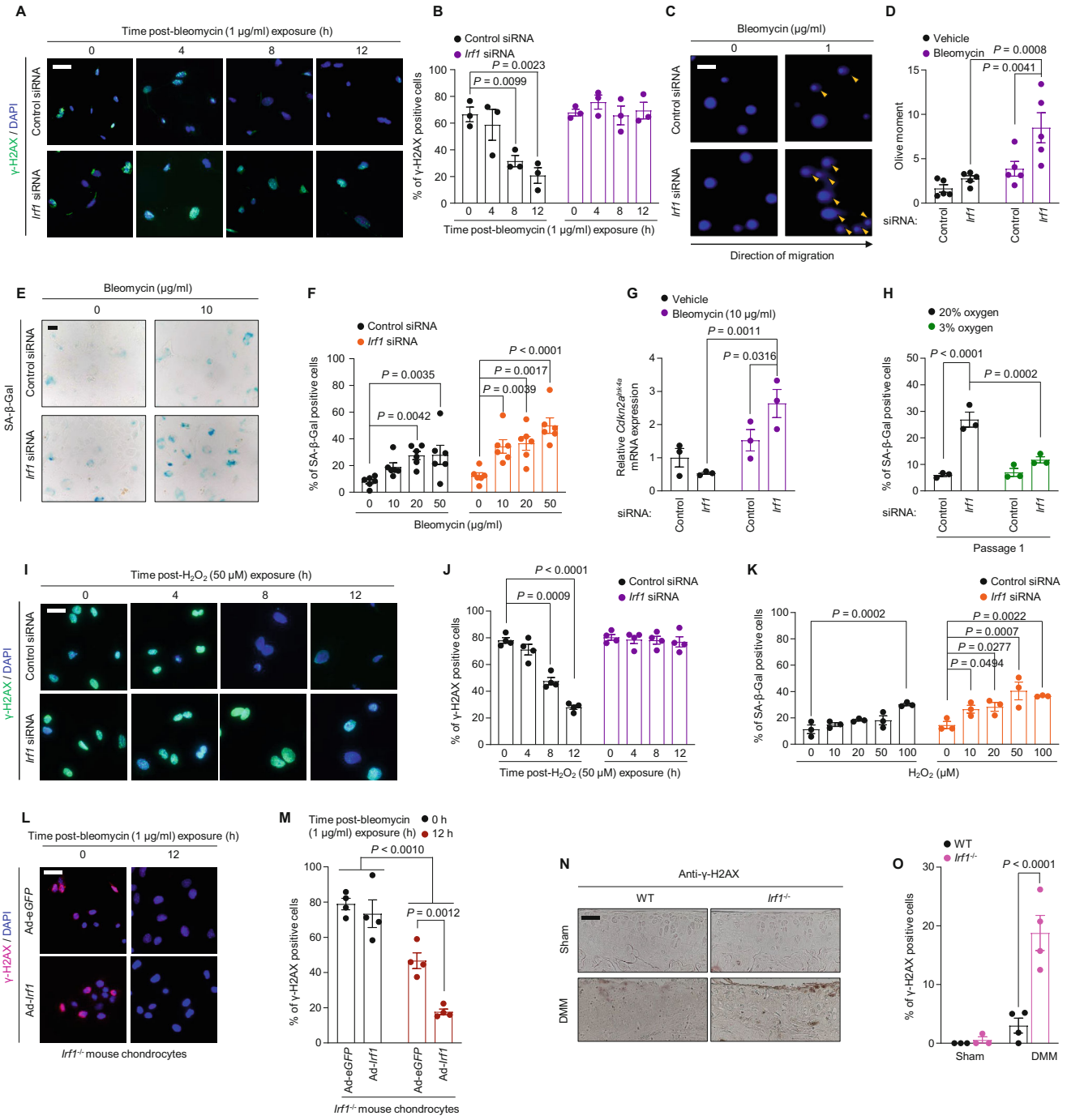


Figure 5. The role of IRF1 in preventing DNA damage accumulation and senescence in chondrocytes. (A–G) Chondrocytes, transfected with indicated siRNAs, were treated with bleomycin. Representative images of γ-H2AX immunofluorescence at the indicated time points (A) and quantification (n = 3) (B) are shown. Representative images of comet assay (C) and olive moments quantification (n = 5) (D) are shown. Yellow arrowheads represent migration of damaged DNA streak. SA-β-Gal staining (E) and quantitation (n = 6) (F) are shown. (G) Relative *Cdkn2a*^{Ink4a} expression (n = 3) is shown. (H) Quantitation of SA-β-Gal staining in mouse chondrocytes treated with indicated siRNAs cultured under normoxia or hypoxia (n = 3) is shown. (I–K) siRNA-transfected chondrocytes were treated with H_2O_2. Representative γ-H2AX immunofluorescence (I) and quantification (n = 4) (J) are shown. (K) Quantitation of SA-β-Gal-positive chondrocytes (n = 3) is shown. (L and M) *Irf1*$^{-/-}$ chondrocytes, infected with Ad-e*GFP* or Ad-*Irf1*, were treated with bleomycin. γ-H2AX immunofluorescence (L) and quantification (n = 4) (M) are shown. Representative images of γ-H2AX IHC in knee joint from sham- or DMM-operated WT and *Irf1*$^{-/-}$ mice six weeks post-surgery (N) and quantification (n = 3) (O) are shown. Data are presented as the mean ± SEM. *P* values for (B), (D), (F–H), (J), (K), (M), and (O) were obtained using ANOVA followed by Fisher's LSD test. Scale bars: 50 μm (A, C, E, I, L, and N). h, hour; Ad-e*GFP*, adenovirus expressing enhanced green fluorescent protein; ANOVA, analysis of variance; DMM, destabilization of the medial meniscus; IHC, immunohistochemistry; IRF1, interferon regulatory factor 1; LSD, least significant difference; mRNA, messenger RNA; SA-β-Gal, senescence-associated beta-galactosidase; siRNA, small interfering RNA; WT, wild-type.

RIGHTSLINK

23265305, 2024, 6, Downloaded from https://acrjournals.onlinelibrary.wiley.com/doi/10.1002/art.42815 by Ewha Womans University Library, Wiley Online Library on [30/10/2024]. See the Terms and Conditions (https://onlinelibrary.wiley.com/terms-and-conditions) on Wiley Online Library for rules of use; OA articles are governed by the applicable Creative Commons License

time, leading to the persistent accumulation of DNA damage. They were prone to cellular senescence even at 10-fold lower doses of H_2O_2 in contrast to the control siRNA–treated chondrocytes, which were resistant to entering a state of senescence until they were exposed to a high dose of H_2O_2 (100 μM) (Figure 5K). IRF1 overexpression through the adenoviral system effectively rescued DNA repair capacity, which had been compromised in *Irf1*$^{-/-}$ chondrocytes (Figure 5L and M). Moreover, the overexpression of IRF1 prevented the accumulation of DNA damage and the entry into senescence elicited by bleomycin treatment in WT chondrocytes (Supplementary Figure 5B–E). Combined with our results in post-traumatic OA models of *Irf1*$^{-/-}$ mice (Figure 3 and Supplementary Figure 3), we demonstrate that IRF1 is required for managing DNA repair in chondrocytes (Figure 5N and O) such that its deficiency promotes chondrocyte senescence, promoting SASP expression, and accelerating OA progression.

DISCUSSION

IRF1 is an immunomodulatory TF that functions in antiviral responses,[28,29] autoimmunity,[5,30] and immunologic development.[31] The conventional notion suggests that the targeted inhibition of IRF1 is a potential therapeutic approach for controlling inflammatory diseases such as rheumatoid arthritis.[32,33] In the meantime, with advances in the genome-wide discovery of TF and DNA interactions, the binding of IRF1 to the cis-acting elements of DNA repair genes has been noted.[34] IRF1 expression was required to mediate the repair of DNA interstrand crosslink damages in cellular contexts. However, it is unknown to date whether the noncanonical function of IRF1 in the DNA damage response has any physiologic significance or whether it is an unconventional response exclusively observed in cell culture conditions.

There is an emerging notion that OA is a disease caused by a metabolic shift in redox homeostasis.[11,13,14,35,36] The resulting oxidative stress causes permanent DNA damage in the chondrocytes, thereby promoting their entry into senescence.[10–14] Senescent chondrocytes serve as a source of chronic inflammation in joints by expressing SASP factors, including proinflammatory cytokines, chemokines, and proteases.[15] Here, we demonstrated that the primary role of IRF1 in cartilage is associated with its noncanonical contribution to mediating the DNA damage response under continual stress conditions in the articular joint (Supplementary Figure 5F). IRF1 predominantly occupies the promoters of DNA repair genes in chondrocytes. Chondrocytes lacking IRF1 expression are left with irreversible DNA damage under oxidative stress, which facilitates their entry into cellular senescence. Genetic deletion of *Irf1* in mice causes accumulation of senescent chondrocytes in the cartilage and accelerates the progression of post-traumatic OA. Therefore, IRF1 is an essential regulator of the DNA repair machinery in chondrocytes.

Our findings indicate an elevation in mechanical allodynia associated with OA in *Irf1*$^{-/-}$ mice. SASP factors produced in joint microenvironments are crucial in eliciting OA-associated neuropathic pain,[15,37] as further evidenced by pain relief in OA joints after the senolytic removal of senescent cells. In fact, SASP factors, including *Mmp3* and *Vegfb*,[15,38] exhibited elevated levels in chondrocytes after IRF1 knockdown, and these factors have been mechanistically linked to the onset of mechanical allodynia associated with OA.[15] Therefore, the induction in SASP levels observed in *Irf1*$^{-/-}$ mice may serve as a contributing factor to the observed pain aggravation in these mice. Furthermore, the production of extracellular matrix fragments within the joint has been linked to mechanical allodynia in joints. Notably, mice lacking matrix-degrading enzymes demonstrate resistance to the development of mechanical allodynia.[39] Consequently, *Irf1*$^{-/-}$ mice, which display the increased extent of cartilage degradation, may be predisposed to experiencing heightened mechanical allodynia in their joints.

We demonstrate that IRF1 expression is down-regulated in the OA cartilage of both human patients and mouse models of post-traumatic OA. Our findings suggest that IRF1 is primarily regulated at the transcriptional level, as supported by the consistent reduction in its transcript levels in the publicly available transcriptome data set from both human patients with OA and post-traumatic OA mouse models. Nevertheless, it should be noted that IRF1 is subjected to a variety of regulatory mechanisms, encompassing both transcriptional[40] and post-translational processes, which include sumoylation.[41] Therefore, a more comprehensive understanding of the precise regulatory mechanisms governing IRF1 in osteoarthritic cartilage warrants further investigation.

A limitation of our study is that we used whole-body *Irf1*$^{-/-}$ mice, although we primarily investigated the role of IRF1 in chondrocytes. As a result, we cannot entirely rule out the possibility that IRF1 deficiency in other cell types comprising the joints may contribute to augmented OA phenotypes in *Irf1*$^{-/-}$ mice. Furthermore, although we did not observe any external developmental defects in the musculoskeletal system of *Irf1*$^{-/-}$ mice, compensatory pathways in response to *Irf1* knockout may have affected the in vivo phenotypes. Future investigations can address these limitations by generating transgenic animals that contain the floxed *Irf1* and cre recombinase fused to a mutant estrogen ligand-binding domain (CreER) driven by *Col2a1*, *Acan*, or *Sox9* promoters to specifically delete *Irf1* in the chondrocytes of adult mice. Nevertheless, it is important to note that therapeutic modalities to treat OA are still administered systemically or through IA injection, affecting multiple cell types in the body or joints, respectively. Thus, our finding that global deficiency of IRF1 exacerbates OA phenotypes provides a critical caveat in using pharmacological approaches that interfere with IRF1 activity.

RIGHTSLINK

23265205, 2024, 6, Downloaded from https://acrjournals.onlinelibrary.wiley.com/doi/10.1002/art.42815 by Ewha Womans University Library, Wiley Online Library on [30/10/2024]. See the Terms and Conditions (https://onlinelibrary.wiley.com/terms-and-conditions) on Wiley Online Library for rules of use; OA articles are governed by the applicable Creative Commons License

Risk factors for OA, such as age, obesity, and joint instability, have been linked to ROS generation in joints.[42–44] The lack of continuous surveillance of oxidative DNA damage renders chondrocytes vulnerable to cellular senescence and drives OA development. We propose an unrecognized, chondroprotective function of IRF1 that has substantial and immediate implications for designing therapies and preventive medicines to limit OA progression.

ACKNOWLEDGMENTS

We thank the staff of the orthopedic surgery teams of Seoul National University Boramae Hospital and Seoul National University Bundang Hospital and the patients for participating in the study.

AUTHOR CONTRIBUTIONS

All authors were involved in drafting the article or revising it critically for important intellectual content, and all authors approved the final version to be published. Dr Kim had full access to all of the data in the study and takes responsibility for the integrity of the data and the accuracy of the data analysis.

Study conception and design. Cho, H. Kim, Yook, Jin-Hong Kim.
Acquisition of data. Cho, H. Kim, Yook, Yong, S. Kim, N. Lee.
Analysis and interpretation of data. Cho, H. Kim, Yook, Yong, S. Kim, N. Lee, Y.-J. Kim, Jin-Hee Kim, T. W. Kim, M. J. Chang, K. M. Lee, C. B. Chang, Kang, Jin-Hong Kim.

Data availability

The transcriptome data sets of siRNA–treated mouse chondrocytes (GSE230800), adenovirus-treated mouse chondrocytes (GSE252509), and the ATAC-seq data set (GSE230796) have been deposited in the Gene Expression Omnibus. All data are contained within the article and its online Supplementary Material.

REFERENCES

1. Honda K, Takaoka A, Taniguchi T. Type I interferon [corrected] gene induction by the interferon regulatory factor family of transcription factors. Immunity 2006;25(3):349–360.
2. Liu-Bryan R, Terkeltaub R. Emerging regulators of the inflammatory process in osteoarthritis. Nat Rev Rheumatol 2015;11(1):35–44.
3. Venkatesh D, Ernandez T, Rosetti F, et al. Endothelial TNF receptor 2 induces IRF-1 transcription factor-dependent interferon-beta autocrine signaling to promote monocyte recruitment. Immunity 2013;38(5):1025–1037.
4. Wang Q, Yu X, Gong M. Single-cell transcriptome analysis reveals the importance of IRF-1/FSTL1 in synovial fibroblast subsets for the development of rheumatoid arthritis. Comput Math Methods Med 2022;2022:1169614.
5. Bonelli M, Dalwigk K, Platzer A, et al. IRF-1 is critical for the TNF-driven interferon response in rheumatoid fibroblast-like synoviocytes. Exp Mol Med 2019;51(7):75.
6. Tada Y, Ho A, Matsuyama T, et al. Reduced incidence and severity of antigen-induced autoimmune diseases in mice lacking interferon regulatory factor-1. J Exp Med 1997;185(2):231–238.
7. Robinson WH, Lepus CM, Wang Q, et al. Low-grade inflammation as a key mediator of the pathogenesis of osteoarthritis. Nat Rev Rheumatol 2016;12(10):580–592.
8. Aigner T, Soder S, Gebhard PM, et al. Mechanisms of disease: role of chondrocytes in the pathogenesis of osteoarthritis–structure, chaos and senescence. Nat Clin Pract Rheumatol 2007;3(7):391–399.
9. Koike M, Nojiri H, Ozawa Y, et al. Mechanical overloading causes mitochondrial superoxide and SOD2 imbalance in chondrocytes resulting in cartilage degeneration. Sci Rep 2015;5:11722.
10. Kang D, Shin J, Cho Y, et al. Stress-activated miR-204 governs senescent phenotypes of chondrocytes to promote osteoarthritis development. Sci Transl Med 2019;11(486):eaar6659.
11. Kang D, Lee J, Jung J, et al. Selenophosphate synthetase 1 deficiency exacerbates osteoarthritis by dysregulating redox homeostasis. Nat Commun 2022;13(1):779.
12. Liu Y, Zhang Z, Li T, et al. Senescence in osteoarthritis: from mechanism to potential treatment. Arthritis Res Ther 2022;24(1):174.
13. Cornelis FMF, Monteagudo S, Guns LKA, et al. ANP32A regulates ATM expression and prevents oxidative stress in cartilage, brain, and bone. Sci Transl Med 2018;10(458):eaar8426.
14. Coryell PR, Diekman BO, Loeser RF. Mechanisms and therapeutic implications of cellular senescence in osteoarthritis. Nat Rev Rheumatol 2021;17(1):47–57.
15. Jeon OH, David N, Campisi J, et al. Senescent cells and osteoarthritis: a painful connection. J Clin Invest 2018;128(4):1229–1237.
16. Wu CJ, Liu RX, Huan SW, et al. Senescent skeletal cells cross-talk with synovial cells plays a key role in the pathogenesis of osteoarthritis. Arthritis Res Ther 2022;24(1):59.
17. Kilkenny C, Browne WJ, Cuthill IC, et al. Improving bioscience research reporting: the ARRIVE guidelines for reporting animal research. Osteoarthritis Cartilage 2012;20(4):256–260.
18. Glasson SS, Blanchet TJ, Morris EA. The surgical destabilization of the medial meniscus (DMM) model of osteoarthritis in the 129/SvEv mouse. Osteoarthritis Cartilage 2007;15(9):1061–1069.
19. Jeon OH, Kim C, Laberge RM, et al. Local clearance of senescent cells attenuates the development of post-traumatic osteoarthritis and creates a pro-regenerative environment. Nat Med 2017;23(6):775–781.
20. Little CB, Barai A, Burkhardt D, et al. Matrix metalloproteinase 13-deficient mice are resistant to osteoarthritic cartilage erosion but not chondrocyte hypertrophy or osteophyte development. Arthritis Rheum 2009;60(12):3723–3733.
21. Ryu JH, Yang S, Shin Y, et al. Interleukin-6 plays an essential role in hypoxia-inducible factor 2α-induced experimental osteoarthritic cartilage destruction in mice. Arthritis Rheum 2011;63(9):2732–2743.
22. Xiang Y, Laurent B, Hsu CH, et al. RNA m^6A methylation regulates the ultraviolet-induced DNA damage response. Nature 2017;543(7646):573–576.
23. Chen H, Yang H, Zhu X, et al. m^5C modification of mRNA serves a DNA damage code to promote homologous recombination. Nat Commun 2020;11(1):2834.
24. Feng L, Wang J, Chen J. The Lys63-specific deubiquitinating enzyme BRCC36 is regulated by two scaffold proteins localizing in different subcellular compartments. J Biol Chem 2010;285(40):30982–30988.
25. Brandl A, Hartmann A, Bechmann V, et al. Oxidative stress induces senescence in chondrocytes. J Orthop Res 2011;29(7):1114–1120.
26. Rodier F, Coppe JP, Patil CK, et al. Persistent DNA damage signalling triggers senescence-associated inflammatory cytokine secretion. Nat Cell Biol 2009;11(8):973–979.
27. Lafont JE. Lack of oxygen in articular cartilage: consequences for chondrocyte biology. Int J Exp Pathol 2010;91(2):99–106.

RIGHTSLINK

23265205, 2024, 6, Downloaded from https://acrjournals.onlinelibrary.wiley.com/doi/10.1002/art.42815 by Ewha Womans University Library, Wiley Online Library on [30/10/2024]. See the Terms and Conditions (https://onlinelibrary.wiley.com/terms-and-conditions) on Wiley Online Library for rules of use; OA articles are governed by the applicable Creative Commons License

28. Panda D, Gjinaj E, Bachu M, et al. IRF-1 maintains optimal constitutive expression of antiviral genes and regulates the early antiviral response. Front Immunol 2019;10:1019.
29. Feng H, Lenarcic EM, Yamane D, et al. NLRX1 promotes immediate IRF-1-directed antiviral responses by limiting dsRNA-activated translational inhibition mediated by PKR. Nat Immunol 2017;18(12): 1299–1309.
30. Matta B, Song S, Li D, et al. Interferon regulatory factor signaling in autoimmune disease. Cytokine 2017;98:15–26.
31. Karwacz K, Miraldi ER, Pokrovskii M, et al. Critical role of IRF-1 and BATF in forming chromatin landscape during type 1 regulatory cell differentiation. Nat Immunol 2017;18(4):412–421.
32. Shiraishi A, Dudler J, Lotz M. The role of IFN regulatory factor-1 in synovitis and nitric oxide production. J Immunol 1997;159(7):3549–3554.
33. Lohoff M, Mak TW. Roles of interferon-regulatory factors in T-helper-cell differentiation. Nat Rev Immunol 2005;5(2):125–135.
34. Frontini M, Vijayakumar M, Garvin A, et al. A ChIP-chip approach reveals a novel role for transcription factor IRF-1 in the DNA damage response. Nucleic Acids Res 2009;37(4):1073–1085.
35. Coleman MC, Goetz JE, Brouillette MJ, et al. Targeting mitochondrial responses to intra-articular fracture to prevent posttraumatic osteoarthritis. Sci Transl Med 2018;10(427):eaan5372.
36. Arra M, Swarnkar G, Ke K, et al. LDHA-mediated ROS generation in chondrocytes is a potential therapeutic target for osteoarthritis. Nat Commun 2020;11(1):3427.
37. Miller RE, Tran PB, Das R, et al. CCR2 chemokine receptor signaling mediates pain in experimental osteoarthritis. Proc Natl Acad Sci U S A 2012;109(50):20602–20607.
38. Vinatier C, Dominguez E, Guicheux J, et al. Role of the inflammation-autophagy-senescence integrative network in osteoarthritis. Front Physiol 2018;9:706.
39. Malfait AM, Ritchie J, Gil AS, et al. ADAMTS-5 deficient mice do not develop mechanical allodynia associated with osteoarthritis following medial meniscal destabilization. Osteoarthritis Cartilage 2010;18(4): 572–580.
40. Forero A, Ozarkar S, Li H, et al. Differential activation of the transcription factor IRF-1 underlies the distinct immune responses elicited by type i and type iii interferons. Immunity 2019;51(3):451–464.e6.
41. Park J, Kim K, Lee EJ, et al. Elevated level of SUMOylated IRF-1 in tumor cells interferes with IRF-1-mediated apoptosis. Proc Natl Acad Sci U S A 2007;104(43):17028–17033.
42. Furukawa S, Fujita T, Shimabukuro M, et al. Increased oxidative stress in obesity and its impact on metabolic syndrome. J Clin Invest 2004; 114(12):1752–1761.
43. Loeser RF, Collins JA, Diekman BO. Ageing and the pathogenesis of osteoarthritis. Nat Rev Rheumatol 2016;12(7):412–420.
44. Loeser RF. Aging and osteoarthritis. Curr Opin Rheumatol 2011; 23(5):492–496.

23265205, 2024, 6, Downloaded from https://acrjournals.onlinelibrary.wiley.com/doi/10.1002/art.42815 by Ewha Womans University Library, Wiley Online Library on [30/10/2024]. See the Terms and Conditions (https://onlinelibrary.wiley.com/terms-and-conditions) on Wiley Online Library for rules of use; OA articles are governed by the applicable Creative Commons License

RIGHTSLINK